

CHAPTER II**THEORETICAL BACKGROUND FOR X-RAY WORK.**

25

2.1. Introduction

In the references¹⁻⁴ the X-ray diffraction studies of liquid crystals have been reviewed and the detailed theoretical considerations are given in references⁵⁻⁶. From X-ray diffraction study we can get idea about molecular interactions in liquid crystals. First attempt was made by Lingen⁷ and Friedel⁸. Generally nematic liquid crystals samples consist of a large number of domains, the molecules are ordered within each domain in a preferred direction (director \vec{n}) but there is no preferred direction for the specimen as a whole. So the X-ray diffraction pattern has a symmetry of revolution around the direction of the X-ray beams. It is evident from the uniform halo just like that of an isotropic liquid. Diffraction photographs of the sample oriented by some means are therefore, needed to specify the state of ordering. With the help of intensity distribution in the equatorial plane of the diffraction pattern (oriented) one can obtain the cylindrical distribution function, giving the probability of finding two atoms at a particular distance, the atoms however, may belong to same or different molecules. Moreover, according to Chistyakov³, the method involves an integration over the scattering vector from zero to infinity which can never be fulfilled by photographic methods with a flat plate camera, the plate being normal to the X-ray beam. Calculation of cylindrical distribution

function and order parameters from X-ray diffraction works has been done by de Vries⁹, while orientational distribution function and order parameters have been calculated by various workers¹⁰⁻¹⁴.

2.2. Average Intermolecular Distance, Apparent length of the Molecules and Layer Thickness (in case of smectic)

In general it is possible to calculate a spacing X , from the position of a diffraction maxima by a formula of the type

$$2X \sin \alpha = K_1 n \lambda \quad \dots(1)$$

Here 2α is the diffraction angle measured between the incident and diffracted beams, n is the order of reflection, K_1 is a constant depending on the shape and arrangement of the molecule.

De Vries has discussed the equations and, their applications and their limit in details^{15,16}. We used $K = 1$ in equation (1) for determining the apparent molecular length.

For both the oriented and un-oriented samples we have used $K = 1.117$ to calculate the intermolecular distance (D). This is because of the fact that, considering the π scattering from a pair of molecules of a distance D apart, if the chains are allowed to rotate freely around each other, the positions of the maxima along the equator are determined by the function¹⁵,

$$J_0(x) = \int_0^{2\pi} \cos(x \cos \alpha) d\alpha$$

271

where $X = \frac{4\pi}{\lambda} \cdot D \sin \alpha$ and this gives for first maxima $K_1 = 1.117$.

Wendorff et al¹⁷ calculated K values from the photograph of some cholesterol esters by taking X values in eqn. (1) from completely extended form of the molecules and found that K lies between 1 for perfectly order molecule and 1.229 for random orientation of the molecules.

2.3. Orientational distribution functions and order parameters.

For a system of cylindrically symmetric molecules one can define an orientational distribution function $f(\beta)$ depending on the angle between the molecular symmetry axis and the directors¹⁴, which gives an average states of orientation of the long axis of the molecules. The X-ray diffraction photographs record intensities averaged over a sufficiently long time and over a sufficiently large volume, so the molecules may be assumed to have an average cylindrical symmetry, even if they are not rotating about their long axes⁴. For a system of rigid rods the order parameters $\langle P_2 \rangle$ and $\langle P_4 \rangle$ may be defined by

$$\langle P_L \rangle = \frac{\int_0^{\pi/2} P_L(\cos\beta) f(\beta) \sin\beta d\beta}{\int_0^{\pi/2} f(\beta) \sin\beta d\beta} \dots(2)$$

where L = 2 and 4; $P_L(\cos\beta)$ is a well known Legendre polynomial of order L. Leadbetter et al^{11,12} reported the measurements of $f(\beta)$, by X-ray method.

(28)

In relating the X-ray intensities $I(\psi)$ around the diffuse equatorial arc (Fig. 2.1) with the orientational distribution function, Leadbetter and Norris¹¹ assumed the molecules as rigid rods perfectly aligned in a cluster of a small number of molecules and obtained

$$I(\psi) = c \int_{\beta=\psi}^{\pi/2} f_d(\beta) \sec^2\psi [\tan^2\beta - \tan^2\psi]^{-\frac{1}{2}} \sin\beta d\beta \quad \dots(3)$$

where $f_d(\beta)$ describes the distribution function of the clusters in which the molecules are perfectly aligned.

They also assumed that for a perfect aligned sample

$$[f_d(\beta) = \delta(\beta)] \quad , \quad \text{the scattering is zero}$$

except for the directions of the scattering vector perpendicular to cluster axis. They have however, calculated

the effects and shown that the deviations are negligible except for highly ordered, phases ($\langle P_2 \rangle \geq 0.8$).

Further comparing the values $f_d(\beta)$ with $f(\beta)$ of the same samples obtained by other methods they have shown that the values of $f_d(\beta)$ is same as that of the true singlet orientational distribution function.

Because of the molecular distribution in the nematic phase centro-symmetric, the distribution function and intensity distribution function can be expanded in the form^{11,18}

$$I(\psi) = \sum_{n=0}^{\infty} a_{2n} \cos^{2n}\psi \quad \dots(4)$$

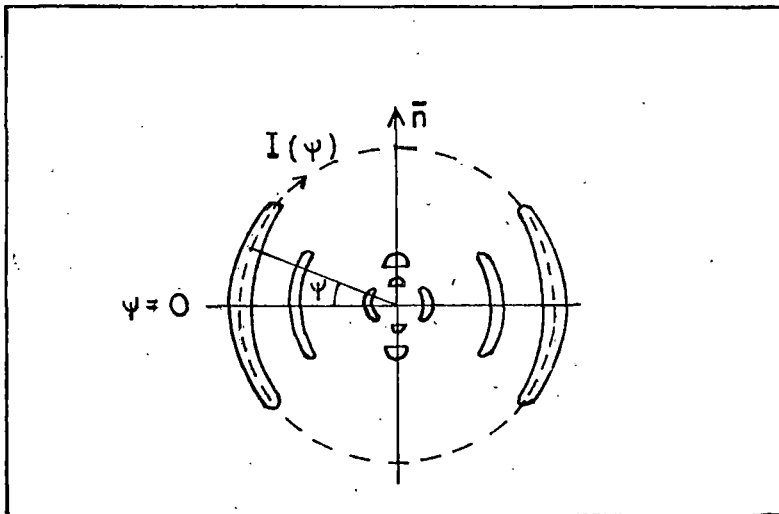


Fig. 2.1. Schematic representation of the X-ray diffraction photograph of an oriented liquid crystal.

$$f(\beta) = \sum_{n=0}^r b_{2n} \cos^{2n} \beta \quad \dots(5)$$

In eqn. (2) by substituting $\sin \alpha = \cos \beta \sec \psi$ we get,

$$I(\psi) = c_0 \int_0^{\pi/2} f_1(\alpha) \sin \alpha d\alpha \quad \dots(6)$$

From eqn. (3), (4) and (5) we get,

$$\begin{aligned} \sum_{n=0}^r a_{2n} \cos^{2n} \psi &= \int_0^{\pi/2} \sum_{n=0}^r b_{2n} \cos^{2n} \psi \sin^{2n+1} \alpha d\alpha \\ &= \sum_{n=0}^r b_{2n} \cos^{2n} \psi \int_0^{\pi/2} \sin^{2n+1} \alpha d\alpha \end{aligned} \quad \dots(7)$$

As ψ is arbitrary, the coefficients of $\cos^{2n} \psi$ must be equal. Now

$$\int_0^{\pi/2} \sin^{2n+1} \alpha d\alpha = \frac{2^n (n!)^2}{(2n+1)!}$$

so

$$b_{2n} = a_{2n} \frac{(2n+1)!}{2^{2n} (n!)^2} \quad \dots(8)$$

The series in eqn. (4) and (5) converges rapidly. Keeping eight terms in the truncated series, a least square fitting is made to obtain the coefficients from

31

eqn. (4) with the corrected experimental intensity values. We find the calculated intensity values agreed with the observed values in all cases. These values of a_{2n} are then used to calculate the coefficients b_{2n} in the truncated series for $f(\beta)$ in eqn. (5) with the help of eqn. (8) $f(\beta)$ is then calculated using eqn.(5).

By calculating the integral

$$\int_0^{\pi/2} f(\beta) \sin\beta d\beta = K \quad \text{say}$$

and then dividing all the b_{2n} values by K we obtain the normalised values of the orientational distribution function so that now

$$\int_0^{\pi/2} f(\beta) \sin\beta d\beta = 1 \quad \dots(9)$$

Substituting eqn.(4) in eqn.(1)

$$\langle P_2 \rangle = \frac{1}{2} \frac{\int_0^1 (3e\cos^2\beta - 1) \sum_{n=0}^p b_{2n} \cos^{2n}\beta d(\cos\beta)}{\int_0^1 \sum_{n=0}^p b_{2n} \cos^{2n}\beta d(\cos\beta)} \quad \dots(10)$$

This can be written in terms of standard integrals and

$\langle P_2 \rangle$ can be calculated. Similarly $\langle P_4 \rangle$ also can be calculated.

Vainstein^h 19 obtained a fairly good approximation for the order parameters by replacing $f(\beta)$ values with $I(\psi)$ values keeping the Bragg angle constant in eqn(1).

(32)

We calculated the order parameter value using Vainstein's^h approximation and designated them as $\langle P_2 \rangle_V$ and $\langle P_4 \rangle_V$

2.4. Experimental Technique and Data Analysis.

All the X-ray diffraction photographs were taken in flat plate camera, (Fig. 2.2) fabricated in our laboratory with M/s. Radon House (India) X-ray Unit fitted with copper target. The details of experimental set up has been described by B. Jha et al²⁰. The set up has the high temperature attachment, has the provisions for interchanging collimator, changeable spacer to vary the sample to filament distance and changeable gap between pole pieces of the electromagnet, all the material used are non-magnetic.

The temperatures of the sample was regulated within $\pm 0.5^\circ\text{C}$ by a Indotherm 101, Temperature Controller. The β sample holder was calibrated upto 250°C with known m.p. samples. Strength of the magnetic field between the pole-pieces was measured with a sensitive gaussmeter (ECIL model GH 867). Ni filter of thickness 0.009 was used for all photographs to obtain nearly monochromatic CuK_α radiation of wavelength 1.542 \AA . The Collimator used was of 1 mm. aperture. The exact distance between the film and the sample was determined by taking Aluminium Powder X-ray diffraction pattern. For Al, the unit cell dimension is known, the Bragg angle for hkl reflecting

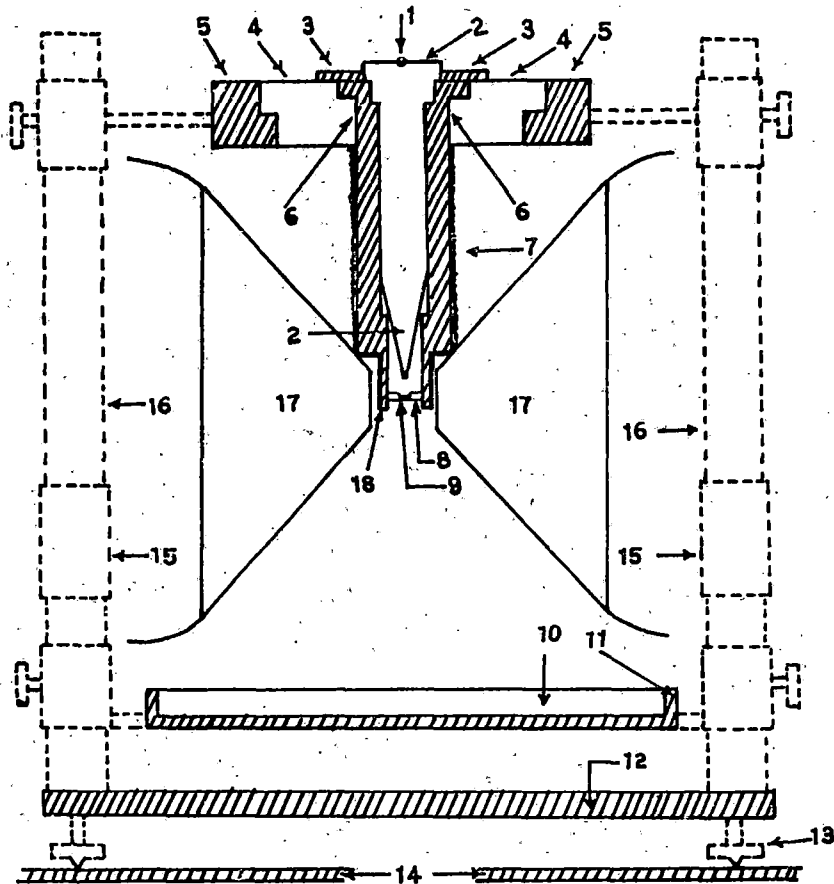


Fig. 2.2: Sectional diagram of the camera:

(1) X-Ray; (2) Collimator; (3) Brass Ring; (4) Ring of Syndanio Board; (5) Brass Ring; (6) Cylindrical Brass Chamber; (7) Asbestos Insulation and Heater Winding; (8) Specimen Holder and Thermocouple; (9) Specimen; (10) Film Cassette; (11) Film Cassette Holder; (12) Base Plate; (13) Levelling Screw; (14) Brass Plates over the Coils of Electromagnet; (15) Removable Spacer; (16) Supporting Brass Stands; (17) Polepieces; (18) Asbestos insulation.

plane can be determined from

$$\sin \theta' = \frac{\lambda}{2a} \sqrt{h^2 + k^2 + l^2} \quad \dots(11)$$

Measuring the diameter of the diffraction ring corresponding to (111) and (200) reflections²¹ the exact distance between the sample and the film can be obtained from the relation

$$\tan 2 \theta' = \frac{\text{Radius of the ring}}{\text{Sample to film distance}} \quad \dots(12)$$

Then the correction term was calculated and applied to the spacer separation to obtain the exact distance.

2.5. Conversion of Optical Density to X-ray Intensity.

The X-ray diffraction photographs were scanned with a Carl Zeiss Microdensitometer (MD 160) both linearly and circularly. The Microdensitometer has potentiometries recording (K200) facility for linear scanning and the circularly scanning was done manually with a rotation stage modified to enable 360° scan by us. The optical density values thus obtained were converted to relative intensity values by a method explained by Flug and Alexander²¹ (Fig. 2.3).

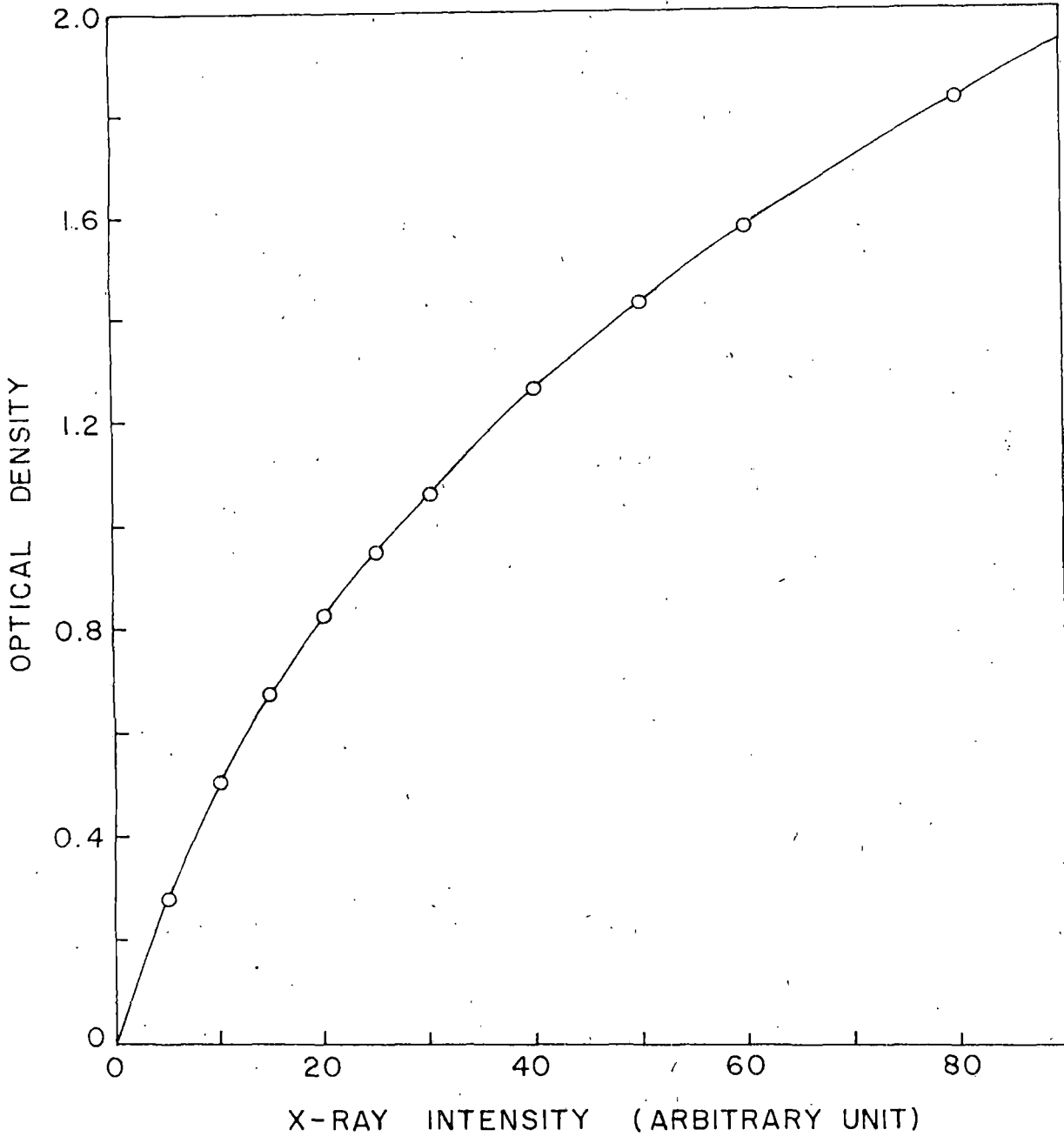


Fig. 2.3

2.6. Linear Scanning and Location of Peak Positions.

A graph relating optical density VS. linear distance is obtained from the linear scan of the outer maxima (Fig. 2.4) through the central spot using the potentiometer recorder. The difference between the peak points of the outer maxima gives its diameter. Peak points can be located by different well known methods (Fig. 2.5), when the peak is well defined we simply take the P_0 position in some cases we used other positions also ($P_{1/2}$, $P_{3/2}$). After knowing the diameter, the Bragg angle corresponding to this diffraction is determined by using eqn. (12) and then average intermolecular distance (D) is calculated using eqn. (1). The same procedure is applied to determine diameter of the inner ring.

Actually in order to get the diameter of the outer crescents accurately, several linear scans were made with different azimuthal angular positions. Considering $I(\psi) \neq 0$ at the maximum intensity ψ position, the linear scan were done for $\psi = 0, \pm 30^\circ$. The mean of the diameters obtained was taken as the actual diameter.

2.7. Circular Scanning and $I(\psi)$ Versus ψ Curves Plotting.

To determine the orientational distribution function $f(\beta)$ and order parameters $\langle P_2 \rangle$ and $\langle P_4 \rangle$ circular scanning is necessary. The values of the optical density obtained from microdensitometric circular scan were converted to X-ray intensities with the help of the calibration

(37)

38

curve. These values were plotted against azimuthal angular position. The correction was done for the background intensity values arising due to the air scattering. The peak intensity position which corresponds to $\psi = 0$ was determined (Fig. 2.6). However, in some cases some unwanted spots for even a slight non-uniformity in film coating create some problems. In such cases a smooth curve was drawn through the large number of points. Symmetric curve around $\lambda = 0$ was drawn very carefully. Mean $I(\psi)$ values of the four quadrants were used to obtain $f(\beta)$, $\langle P_2 \rangle$ and $\langle P_4 \rangle$ values.

Considering nineteen $I(\psi)$ values from $\psi = 0^\circ$ to $\psi = 90^\circ$ at 5° intervals from the smooth $I(\psi)$ vs ψ curve, $f(\beta)$, $\langle P_2 \rangle$ and $\langle P_4 \rangle$ values were calculated by using Leadbetter's approximation. $f(\beta)$ vs β curve was drawn. To perform this calculation a computer program has been developed and used in Nipro Series 8600 Computer.

2.8. Refractive Index

Theoretical considerations -

The birefringence of liquid crystals is the visible manifestation of their long-range order and it is defined only for a uniformly ordered domain. Its value is determined by the degree of order S and by the principal polarizabilities, ϵ_o and ϵ_e for uniaxial systems. These are interrelated by the following equation

39

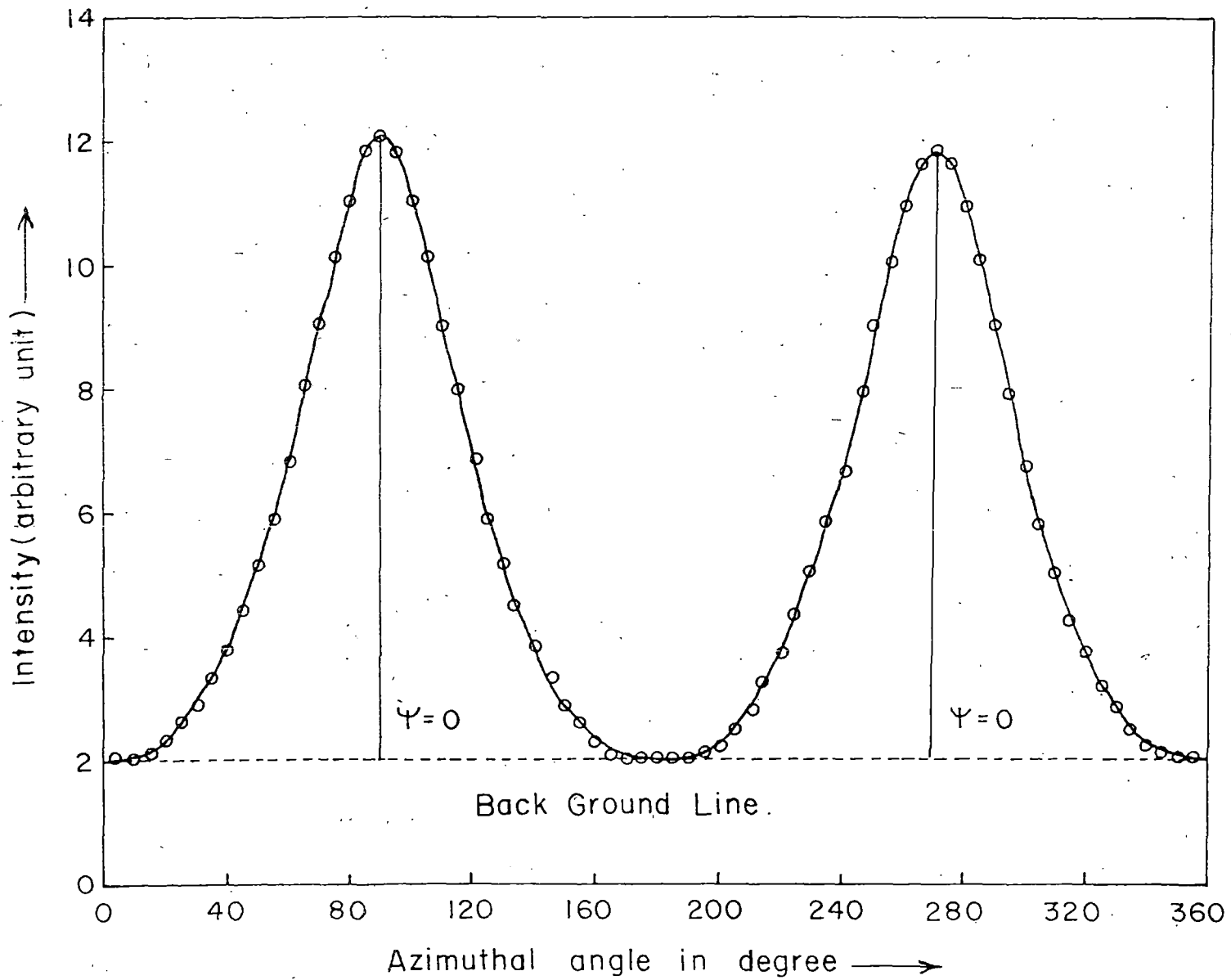


Fig. 2.6

$$S = \frac{(\alpha_e - \alpha_o)_{\text{nematic}}}{(\alpha_e - \alpha_o)_{S=1}} \quad \dots(13)$$

By studying the birefringence we can estimate the orientational ordering in the liquid crystals at different temperatures. Because of the anisotropy of the molecular arrangements in the liquid crystalline phase the well-known Lorentz-Lorentz formula for liquid phase is generally replaced by Vuk's²² formula, Neugebauers' relations²³ or Saupe and Maier anisotropic model²⁴. Chandrasekhar suggested the most comprehensive theory started with the total interaction energy U . We have used both Vuk's and Neugebauer's equations to calculate the polarisabilities

2.9. Vuk's relation

$$(n_o^2 - 1) / (n^2 + 2) = 4\pi N \alpha_o / 3 \quad \dots(14)$$

and

$$(n_e^2 - 1) / (n^2 + 2) = 4\pi N \alpha_e / 3 \quad \dots(15)$$

Neugebauer's equations for calculating the polarisabilities are as follows

$$\frac{1}{\alpha_e} + \frac{2}{\alpha_o} = \frac{4\pi N}{3} \left[\frac{n_e^2 + 2}{n_e^2 + 1} + \frac{2(n_o^2 + 2)}{n_o^2 - 1} \right] \quad \dots(16)$$

and

$$L_e + 2\alpha_o = \frac{9}{4\pi N} \left[\frac{n^2 - 1}{n^2 + 2} \right] \quad \dots(17)$$

Here $n^2 = (2n_o^2 + n_e^2)/3$, n is the mean refractive index and N is the number of molecules per c.c.

The relation between the order parameters and polarizabilities (α_o, α_e) is given by²⁵

$$\begin{aligned}\alpha_e &= \alpha + \frac{2}{3} \alpha_a S \\ \alpha_o &= \alpha - \frac{1}{3} \alpha_a S\end{aligned}$$

where $\alpha = (2\alpha_o + \alpha_e)/3$ is the mean polarizability $\alpha_a = (\alpha_{11} - \alpha_{\perp})$ is the molecular polarizability anisotropy.

$$\text{Therefore } S = \frac{\alpha_e - \alpha_o}{\alpha_{11} - \alpha_{\perp}} \quad \dots(18)$$

To get the value of $(\alpha_{11} - \alpha_{\perp})$ we followed the most widely used Haller's extra polation procedure²⁶.

2.10. Experimental Procedures.

Refractive indices were measured with the help of hollow glass prisms with a refracting angle of about 1° . The prisms are made up of optically flat glass plates. The plates were rubbed parallel to one of their edges they were then treated with 1 percent polyvinyl alcohol solution and then dried. Again they were rubbed along the same direction as before. The prisms were formed keeping the treated surface inside and rubbing directions parallel to the edge of the prism. The prisms were precalibrated by measuring the refractive indices of distilled water and glycerine at different temperatures. They were compared with those measured with Abbe's refractometer.

The liquid crystal samples were allowed to ^{flow} follow in the prism by melting a few crystals at the top. The samples were then cooled very slowly in the presence of magnetic field (0.6 Tesla) applied in the direction of rubbing. The combination of rubbing and flow together with the π magnetic field produced a homogeneous nematic specimen with the optic axis parallel to the edge of the prism. The experimental details of this procedure were given by Zeminder et al.²⁷. The prisms were put inside a brass thermostat heated electrically and controlled by a temperature controller to $\pm 0.5^\circ\text{C}$. A precision spectrometer and a nicol prism were used to measure the refractive indices (n_o, n_e), for different wave lengths. The densities were determined (within $\pm 0.1\%$) by putting weighed samples inside a glass capillary tube which was placed in a water bath heated using a temperature controller. Sufficient time was allowed for attaining the desired temperature. The length of the column was measured by a travelling microscope. The densities were calculated after correcting for the expansion of the glass capillary.

43a

References

1. J. Flaqueirettes and P. Delord; Liquid Crystals and Plastic Crystals. Ed. G.W.Gray and P.A.Dinsor, Vol.2 Ch. 3, Ellis Horwood (1974).
2. H.Kelker and R.Hatz, Hand Book of Liquid Crystals Ch. 5, Verlag Chemie (1980).
3. I.G.Chistyakov; Sov. Phys. Usp. 9, 551 (1967).
4. L.V.Azaroff; Mol.Cryst. Liq.Cryst. 60, 73 (1980).
5. B.K.Vainshtein; Diffraction of X-rays by Chain Molecules; Elsevier Publishing Co., (1966).
6. A.J.Leadbetter; In the Molecular Physics of Liquid Crystals, Ed. G.R.Luckhurst and G.W.Gray, Ch. 13, Academic Press (1979).
7. J.S.V.D.Lingen; Ber.Dt.Chem.Ges. 15, 913 (1913).
8. G.Friedel; Annls.Phys. 18, 273 (1922).
9. A.deVries; J.Chem.Phys. 56, 4489 (1972).
10. P.Delord and J.Falqueirettes, C.r.hebd; Seane. S.Acad. Sci. Paris 260 2468 (1965).
11. A.J.Leadbetter and E.K.Norris; Mol.Phys. 38, No.3, 669 (1979).
12. A.J.Leadbetter and P.G.Wrighton; J.De Physique Collogue, 40 e, 3-234 (1979).
13. B.Bhattacharjee, S.Paul and R.Paul, Mol.Phys. 44,No.6, 1391 (1981).
14. G.Zannoni; The Mol.Phys. of Liquid Crystals, Ed. G.R.Luckhurst and G.W.Gray, Academic Press, Ch.3(1979).

425

15. A. deVries; Mol.Cryst.Liq.Cryst. 10 31 & 219 (1970)
16. A. deVries; Mol.Cryst.Liq.Cryst., 11, 361 (1970), 20 119 (1973).
17. J.K.Wendorff and E.P.Price; Mol.Cryst.Liq.Cryst. 24, 129 (1973).
18. P.G.deGennes; The Physics of Liquid Crystals Ch.2, Oxford (1974).
19. B.K.Vainshtein; Diffraction of X-rays by Chain Molecules, Elsevier, Pub.Co. (1966).
20. B.Jha and R.Paul; Proc.Nucl.Phys.Solid State Physics Symp. India 19c, 491 (1976).
21. H.P.Klug and L.E.Alexander; X-ray Diffraction Procedures; John Wiley and Sons, Ch.3 (1974).
22. M.F.Vuks; Optics and Spectroscopy; 20, 361 (1966)
23. H.E.J. Neugebauer; Canad.J.Phys. 32, 1 (1954).
24. Ref. 23, 24 and 25 of Chapter 1.
25. P.G.de Gennes; Mol.Cryst.Liq.Cryst. 12, 193 (1971).
26. I.Heller, H.A.Huggins, H.R.Lilenthal and T.R.McGuire, J.Phys.Chem.77, 950 (1973).
27. A.K.Zeminder, S.Paul and R.Paul; Mol.Cryst.Liq.Cryst. 61, 191 (1980).